392

Nano Biomed. Eng., 2018, Vol. 10, Iss. 4

Research Article

Effect of the Concentration of NaBH$_4$ and N$_2$H$_4$ as Reductant Agent on the Synthesis of Copper Oxide Nanoparticles and its Potential Antimicrobial Applications

Maribel Guzman[1]✉, Mariella Arcos[2], Jean Dille[3], Stéphane Godet[3], Céline Rousse[4]

[1]Engineering Department, Pontifical Catholic University of Peru, Av. Universitaria 1801, Lima-32, Peru.
[2]Sciences Department, Pontifical Catholic University of Peru, Av. Universitaria 1801, Lima-32, Peru.
[3]4MAT, Université Libre de Bruxelles, CP 194/03, 50 Avenue Roosevelt, B-1050 Brussels, Belgium.
[4]LISM, EA 4695, UFR Sciences Exactes et Naturelles, Université de Reims Champagne-Ardenne, BP 1039, 51687 Reims cedex 2, France.

✉ Corresponding author. E-mail: mguzman@pucp.edu.pe

Abstract

The antibacterial activity of various nanoparticles is gaining increasing interest due to its potential medical applications. In this work, we presented the synthesis of copper oxide nanoparticles prepared by chemical reduction from aqueous solutions of copper sulfate (CuSO$_4$) with sodium borohydride (NaBH$_4$) and hydrazine hydrate (N$_2$H$_4$) as reductant and polyvinylpyrrolidone (PVP) as stabilizer. The X-ray diffraction spectra showed the formation of tenorite (CuO) and cuprite (Cu$_2$O) nanoparticles when different ratios of CuSO$_4$/NaBH$_4$ and CuSO$_4$/N$_2$H$_4$ were used. Photographs obtained by transmission electron microscopy (TEM) showed agglomerates of grains with a narrow size distribution (from 20 to 70 nm), whereas the radii of the individual particles were between 2 and 20 nm. Smaller nanoparticles and narrower particle size distributions were obtained when NaBH$_4$ was used. The results of antibacterial activity using the Kirby-Bauer method showed that nanoparticles obtained with NaBH$_4$ presented a reasonable bactericidal activity. *Pseudomonas aureginosa* and *Staphylococcus aureus* were more susceptible to the particle size than *Escherichia coli*. In addition, with small amounts of Cu$_2$O in samples of CuO nanoparticles, the antibacterial susceptibility against *Pseudomonas aureginosa* was improved. Finally, nanoparticles of CuO incorporated into cotton by applying ultrasound waves remained impregnated after five washes.

Keywords: Chemical reduction; Copper oxide nanoparticles; Antibacterial activity; Nanotechnology; Staphylococcus aureus

Introduction

In recent years, the interest in nanomaterials has increased dramatically due to their unique physical and chemical features. Synthesis of nanosized particles of silver and copper with antibacterial properties is of great interest in the development of new pharmaceutical products [1-3]. Studies on copper

nanoparticles (NPs) have recently attracted increased attention because of their low cost in contrast to gold and silver. In addition, considerable attention is now being directed to transition metal nanostructures based on their metal oxides, which is a crucial step toward realization of functional nanosystems [4]. Bacteriological activity of copper oxide NPs against gram positive (*Staphylococcus aureus* and *Staphylococcus aureus MRSA*) and gram negative (*Escherichia coli* and *Pseudomonas aeruginosa*) strains have been investigated for enhancing antibacterial property [5-14].

Antibacterial activity of the copper oxide NPs can be exploited for disinfection in wastewater treatment plants, to prevent bacteria colonization and to eliminate microorganisms [15]. In addition, deposition of copper oxide NPs on cotton fabric will improve its antibacterial properties. Copper oxide NPs-loaded cotton fabric could be used in medical and textile applications such as medical devices, healthcare, wound dressing, military, protective suits, personal care product, clothing and others [16]. Antimicrobial susceptibility tests have been classified into different methods, based on the applied principle, which include diffusion (Kirby-Bauer and Stokes), dilution (minimum inhibitory concentration), and diffusion & dilution (E-test method). The Kirby-Bauer and Stokes methods are usually used for antimicrobial susceptibility test and the first one is recommended by the National Committee for Clinical Laboratory Standards (NCCLS). This method is well documented and standard zones of inhibition have been determined for susceptible and resistant values [17]. The exact antibacterial action of copper oxide NPs is not completely understood. One of the possible reasons for this behavior could be attributed to a direct interaction between copper oxide NPs and the external membrane surface of the bacteria. Other possible mechanisms involve the interaction of copper oxide with biological macromolecules such as enzymes and DNA through an electron release mechanism [18].

Synthesis of nanosized copper oxide particles with different morphologies and sizes using different routes have been reported [19]. Some methods of synthesis include thermal decomposition [5, 20], calcination [21], pyrolysis [22], sonochemistry [23], electrochemistry [7, 24, 25], microwave irradiation [26-28], precipitation [29-34], reduction [16, 34-40], reverse micelles [41], sol-gel [42] and self-assembled [43, 44]. Along with those methods, the simple process involving a reduction of copper salts has been well developed [30, 45]. This synthetic method involves reduction of an ionic salt in an appropriate medium in the presence of surfactant using various reducing agents as sodium borohydride [37, 38, 46] and hydrazine hydrate [39] as examples.

In this article, we present the synthesis of copper oxide NPs prepared by chemical reduction from aqueous solutions of copper sulphate with sodium borohydride and hydrazine as reductant and polyvinylpyrrolidone (PVP) as a stabilizer.

Experimental
Chemicals and bacterial strains

Cooper sulfate ($CuSO_4$), sodium borohydride ($NaBH_4$), hydrazine hydrate (N_2H_4), ethylenedia-minetetraacetic acid (EDTA, $C_{10}H_{16}N_2O_8$), p otassium hydroxide (KOH), and polyvinylpyrrolidone (PVP-300K) were purchased from Merck. All chemicals were of analytical purity and used as received without further purification. Mili-Q water in all experimental synthesis was used. Gram-positives *Staphylococcus aureus* strain (CCM 3953), *Staphylococcus aureus MRSA strain* (ATCC 9027) and Gram-negatives *Escherichia coli strain* (ATCC 10536), *Pseudomonas aeruginosa strain* (ATCC 10145) were obtained from Universidad Peruana Cayetano Heredia, Peru.

Synthesis of copper oxide nanoparticles (NPs)

Copper oxides NPs were synthesized by modified chemical reduction method proposed by Sayed M. Badawy et al. [47]. Solutions of copper sulfate (18 mM to 40 mM), hydrazine hydrate (60 mM to 100 mM), sodium borohydride (20 mM to 80 mM), EDTA (1.0 mM), potassium hydroxide (2.0 mM) and PVP (0.25-0.75% v/v) were used. The chemical reduction was made at room temperatures. The solution of copper sulfate containing PVP was placed in a 250 mL flask. Then, EDTA and potassium hydroxide solutions were added. Subsequently, the reducing agent solution (hydrazine or sodium borohydride) was gradually dropped into the solution under magnetic stirring at the rate of 3 mL/min at room temperature. The transparent blue color solution gradually turned into opaque blue. Gradually, color of the solution turned dark or red-brown, indicating the formation of copper oxides. The process was carried out for 30 min at

394

Nano Biomed. Eng., 2018,Vol. 10, Iss. 4

room temperature with stirring. After the reaction, the colloids containing NPs were centrifuged at 12 000 rpm for 5 min using a micro centrifuge (Eppendorf 5804). To remove excess copper ions, the copper oxide colloids were washed at least three times with Mili-Q water under nitrogen stream. A dried nanopowder of copper oxides was obtained by freeze-drying. To carry out all the characterization methods and the interaction of copper oxides NPs with bacteria, the copper oxide nanopowder in the freeze-drying cuvette was taken again in suspension in deionized water. The suspension was homogenized with a Fisher Bioblock Scientific ultrasonic cleaning container.

Characterization for copper oxide nanoparticles (NPs)
Structural characterization

X-ray diffraction (XRD) investigation was carried out using BRUKER D8 ADVANCE (Karlsruhe, Germany) X-ray diffractometer equipped with a copper anticathode (l Cu Ka = 1.54056 Å). Data were obtained over the range of $2\theta = 30°\text{-}100°$ using a step size of 0.03° and counting time of 10 sec per step. Reference Intensity Ratio (RIR) method from XRD was used in order to assign the phases observed in the X-ray pattern. Crystallite size measurements were also carried out using the approximate Scherrer equation, $D = k\lambda/\beta \cos\theta$, where D is the crystallite size, k is a constant (= 0.89 assuming that the particles are spherical), λ is the wavelength of the X-ray radiation ($\lambda = 1.54056$ Å), β is the line width at half maximum intensity of the peak, and θ is the angle of diffraction.

Elemental composition analysis

Chemical compositions of the samples were analyzed by scanning electron microscopy using a JEOL JSM 6460LA Scanning Electron Microscope (SEM), coupled with energy-dispersive X-ray spectroscopy (EDS) using an EDXS JEOL 1300 Microprobe.

Transmission electron microscopy

Studies of the size and the morphology of NPs were performed by means of transmission electron microscopy (TEM) using a Philips CM20-Ultra Twin microscope operating at 200 kV. Histograms of the size distribution were calculated from TEM images by measuring the diameters of at least 100 particles using ImageJ software. For preparation of the TEM sample, the nanopowder was dispersed in high-purity ethanol via ultrasonic equipment during 1 min. Then, a few drops of the copper oxide NPs solution were placed on carbon-coated TEM gold grids.

Antibacterial assays of cooper oxides nanoparticles (NPs)

The antimicrobial susceptibility of copper oxide NPs was evaluated using the disc diffusion or Kirby-Bauer method [17]. Zones of inhibition were measured after 24 h of incubation at 35 °C. The comparative stability of discs containing vancomycin and gentamicin was prepared. The standard dilution micro method, determining the minimum inhibitory concentration (MIC) leading to inhibition of bacterial growth, is still under way. However, preliminary results have been obtained.

Coating cotton fabric using cooper oxide nanoparticles (NPs)

The prepared copper oxide nanocrystals were coated onto cotton fibers using ultrasounds. An amount of copper oxide NPs was dispersed in 16 mL Mili-Q water; the colloids were placed in a beaker where ultrasound waves were applied by 10 min. The sample of cotton fibber (11 cm^2 approximately) previously washed with Mili-Q water was placed in the vessel where colloids were suspended. The NPs and the cotton fibber sample were exposed to ultrasound waves for 30 min in a Fisher Bioblock Scientific ultrasonic cleaning container. Cotton fibber samples coated using different copper oxide NPs were subsequently washed with Mili-Q water. The washing waters were collected individually and analyzed by atomic absorption spectroscopy (Atomic Absorption Spectrometer, Varian AA 220) to determine the copper content. Finally, the cotton fibber sample was dried in an oven at 40 °C and prepared for its analysis by SEM and XRD.

Results and Discussion

Copper oxide NPs were synthesized according to the method described in the previous section. Crystalline feature, crystallite size, particle size distribution and morphology by changing various parameters of the synthesized sample were accomplished. First, the effect of sodium borohydride (NaBH$_4$) and hydrazine (N$_2$H$_4$) in the synthesis of NPs was investigated. Then, the morphology and size of NPs were determined. And the antibacterial activity of all copper oxides colloids prepared was examined. Finally, one method to coating
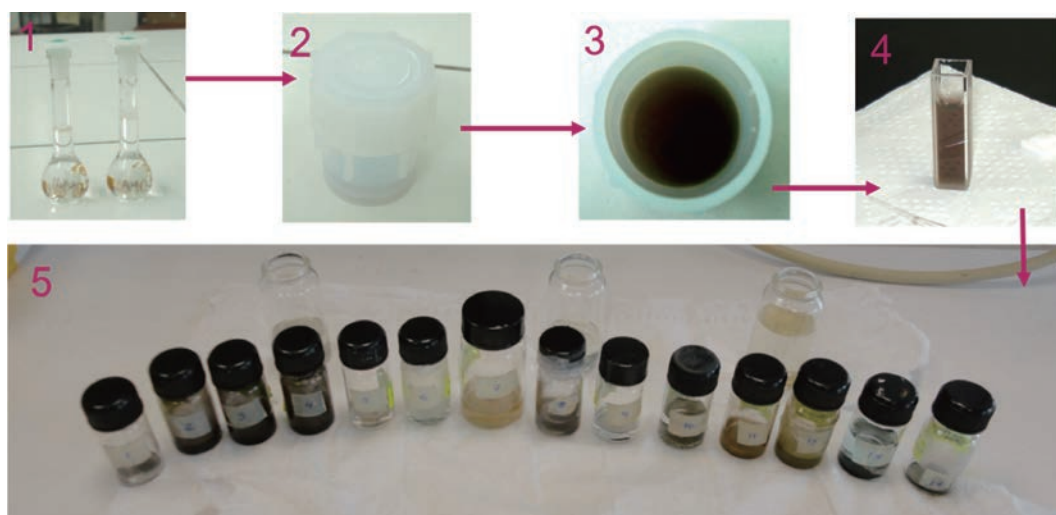
Nano Biomed. Eng., 2018,Vol. 10, Iss. 4

395

Fig. 1 Illustration of the synthesis of copper oxide nanoparticles.

cotton with NPs synthetized was carried out.

Effect of reducing agent

To study the effect of reducing agent, samples using hydrazine and sodium borohydride, both with and without presence of PVP as stabilizing agent were obtained (Fig. 1). The copper oxide colloids obtained showed colors between brown and red if sodium borohydride agent ($NaBH_4$) or hydrazine (N_2H_4) at different concentrations were used. Seven samples at different concentrations were obtained. Details of each sample are showed in Table 1.
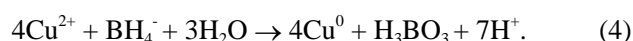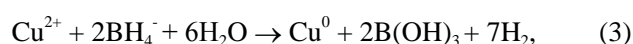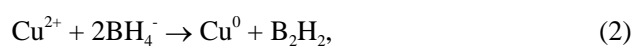
The Cu^{2+} reduction, by N_2H_4 or $NaBH_4$, to copper oxides took place via a number of redox reactions [48]. When the reductant agent is introduced into the aqueous $CuSO_4$ solution, electrons are donated to the Cu^{2+} ions. Although the exact mechanism and reaction route are not very clear yet, a series of redox reactions are assumed during the whole process. In the case of hydrazine (N_2H_4), the reduction is carried out as follows,

Table 1 Ratios of chemical reagents for each sample obtained by chemical reaction (PVP = 0.50% (v/v); EDTA (1.0 mM); KOH (2.0 mM)

Sample	$[Cu^{2+}] : [N_2H_4]$	$[Cu^{2+}] : [NaBH_4]$
MH01	4 : 6	--
MH02	4 : 7	--
MH03	4 : 10	--
MB01	--	4 : 2
MBP01	--	4 : 3
MB02	--	4 : 4
MB03	--	4 : 8

$$2Cu^{2+} + N_2H_2 \rightarrow 2Cu^0 + N_2 + 4H^+. \tag{1}$$
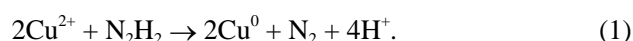
When sodium borohydride ($NaBH_4$) is used, the reduction occurs through electron transfer from borohydride anions to copper ions followed by nucleation of copper atoms. Three mechanisms were proposed [49-51]:

$$Cu^{2+} + 2BH_4^- \rightarrow Cu^0 + B_2H_2, \tag{2}$$

$$Cu^{2+} + 2BH_4^- + 6H_2O \rightarrow Cu^0 + 2B(OH)_3 + 7H_2, \tag{3}$$

$$4Cu^{2+} + BH_4^- + 3H_2O \rightarrow 4Cu^0 + H_3BO_3 + 7H^+. \tag{4}$$

Using either a reducing agent or another, copper NPs obtained could be oxidized into Cu_2O and CuO [49, 52]. Oxidation occurred rapidly as the newly formed copper atoms reacted immediately with dissolved oxygen molecules:

$$4Cu + O_2 \rightarrow 2Cu_2O, \tag{5}$$

$$2Cu + O_2 \rightarrow CuO. \tag{6}$$

However, standard formation enthalpies as of −166.7 kJ/mol and −155.2 kJ/mol indicated that the Cu_2O was slightly more stable than CuO in the solid state. In fact, Chen et al. [53] suggested that an excess of copper NPs could reduce cupric oxide NPs:

$$CuO + Cu \rightarrow Cu_2O. \tag{7}$$

Additionally, under certain conditions of pH[3] 12.5 and temperature, a further oxidation of Cu_2O may occurred:

$$2Cu_2O + O_2 \rightarrow 4CuO. \tag{8}$$

For our working conditions (pH = 10-11), this reaction could not occur. Muramatsu et al. [54] reported that Cu_2O particles could be synthesized from

396

Nano Biomed. Eng., 2018, Vol. 10, Iss. 4

a CuO aqueous suspension using hydrazine as the reducing agent:

$$2N_2H_4 + 2CuO \rightarrow Cu_2O + N_2 + 2NH_3 + H_2O, \qquad (9)$$

$$N_2H_4 + 4CuO \rightarrow 2Cu_2O + N_2 + 2H_2O. \qquad (10)$$
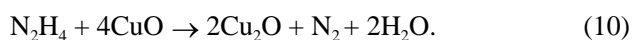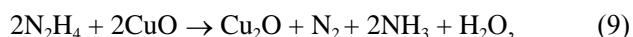
Then, further reduction of CuO NPs can be carried out with abundant amount of hydrazine. On the other hand, Yagi [34] and Zhang et al. [55] reported that Cu_2O NPs could be obtained using $NaBH_4$ if enough amount of PVP in the media was used:

$$4Cu^{2+} + BH_4^- + 5H_2O \rightarrow$$

$$2Cu_2O + B(OH)_3 + 2H_2 + 7H^+. \qquad (11)$$
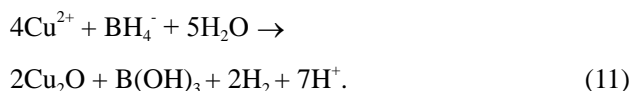
Effect of hydrazine N_2H_4

The elemental analysis of the copper oxide NPs was performed by EDS. Fig.2(a) shows the EDS spectrum of sample MH01. All the K and L emission peaks for copper and oxygen were observed. No other obvious peak belonging to impurity was detected. This result indicated that the as-synthesized product was composed of high-purity copper oxide NPs. A similar EDS spectrum was obtained for the rest of samples prepared using N_2H_4. Fig.2(b) shows the typical powder XRD patterns of the as-prepared MH03 sample. Interplanar distances calculated for (111), (200), (211), (220), (311), (222) and (400) from XRD patterns matched well with standard data, confirming the formation of a single cubic phase of cuprous oxide (Cu_2O) with a cuprite structure (JCPDS card no. 005-0667 space group Pn3m, a = 4.23 Å). No other diffraction peaks arising from Cu, CuO or $CuSO_4$ appeared in the XRD patterns. It was in agreement with results reported previously [20, 23-24, 39, 43-45]. Similar XRD spectra were obtained for the rest of samples when hydrazine was used. This can be due to that all the copper formed (Equation (1)) was oxidized immediately to cuprite according to Equation (5). In addition, it is also
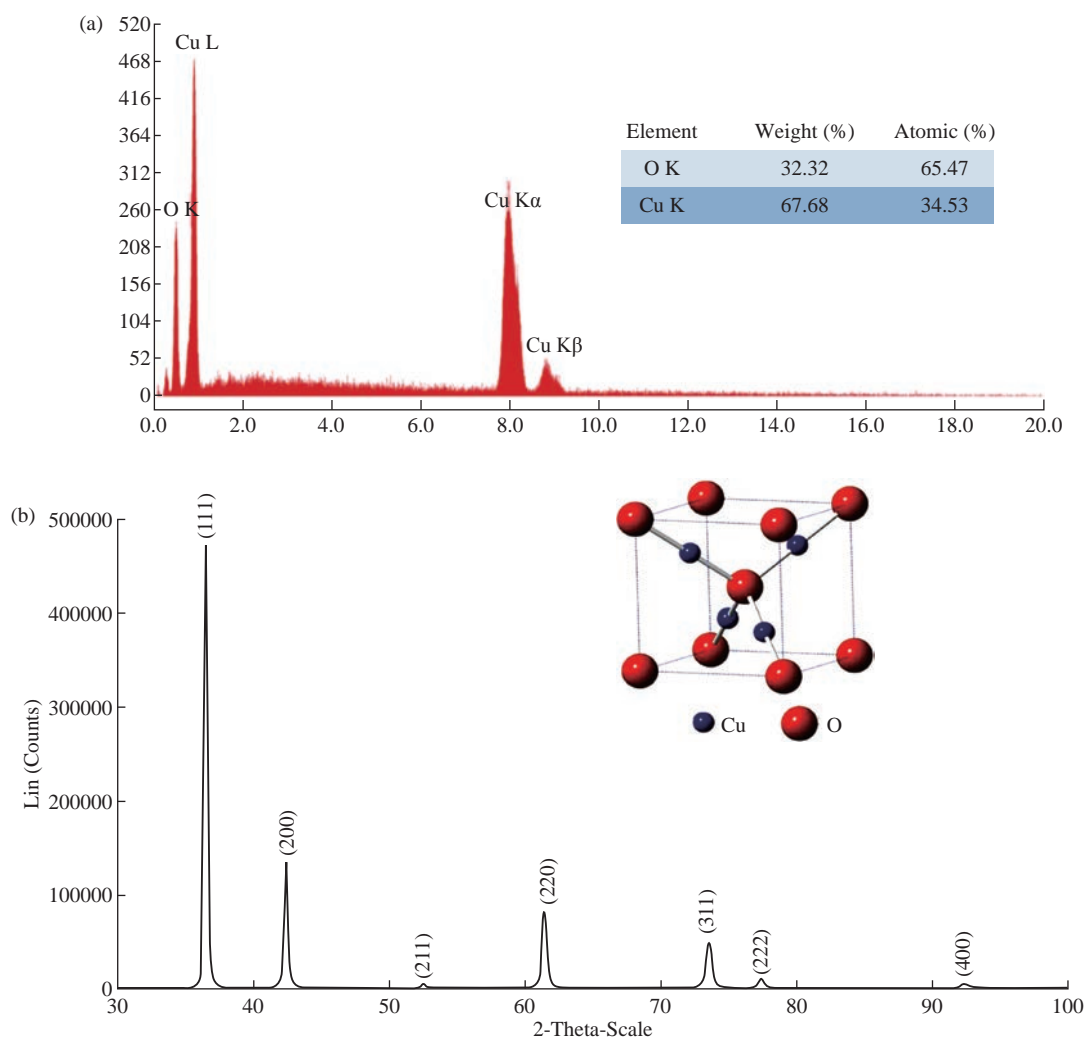

Element	Weight (%)	Atomic (%)
O K	32.32	65.47
Cu K	67.68	34.53

Fig. 2 (a) EDS spectrum of sample copper oxide nanoparticles, $[Cu^{2+}] : [N_2H_4] = 2 : 3$; **(b)** XRD patterns of Cu_2O nanoparticles prepared with hydrazine, $[Cu^{2+}] : [N_2H_4] = 2 : 5$.

Nano Biomed. Eng., 2018, Vol. 10, Iss. 4

397

possible to propose that the concentration of hydrazine is appropriate to reduce any possible tenorite formed according to reactions presented in Equation (9) and (10).

The size and the morphology of copper oxide NPs were analyzed by TEM. Fig. 3 shows the morphology and the particle size distribution of copper oxide NPs when different volumes of reductant agent were used. Fig. 3(a) reveals that the product consisted of well dispersed NPs with a regular morphology and narrow size distribution. Similar results were clearly observed for other two samples prepared using N_2H_4 as reductant agent (Fig. 3(b) and (c)). Semispherical Cu_2O NPs obtained by different ways were previously reported [43, 54-55]. The histograms on the right hand of each picture shows NPs ranging from 3.59 to 19.83 nm, 1.38 to 11.52 nm, and 1.42 to 15.17 nm when the volume of N_2H_4 increased. The estimated mean diameter of 10.85 ± 3.36 nm, 6.81 ± 1.93 nm, and 5.51 ± 1.81 nm was determinate using ImageJ software. Spherical Cu_2O NPs with similar mean diameters were previously reported [20, 24, 37, 40, 56].

It can be observed that as the volume of N_2H_4 increased, the average size of NPs decreased. This can be explained in view that to a greater volume of N_2H_4

the nucleation process of the NPs was favored. As the amount of N_2H_4 increased, the reduction of Cu^{2+} ions and their subsequent nucleation were favored (Equation (1)). Also, it was observed that the dispersion of NPs increased. This may be because the increase of N_2H_4 caused NPs with different sizes to form at the same time, favoring nucleation rather than the growth of NPs. A better understanding of the effect of the ratio of $Cu^{2+} : N_2H_4$ on NP synthesis can be obtained by considering the mechanisms involved in NP formation. According to LaMer et al. [57-58], the mechanism of formation of NPs can be divided into two stages: Nucleation and growth. The results showed that as the N_2H_4 volume increased, the nucleation process was favored until the critical radius was reached, and therefore the mean size of the NPs decreased (Table 2). The crystallite size was also calculated using the approximate Scherrer formula from the width of (111) plane and was found to be 8.89 nm.

Effect of sodium borohydride NaBH₄

The elemental analysis of the copper oxide NPs was performed by EDS. Fig. 4(a) shows the EDS spectrum of sample MB01. All the K and L emission peaks for copper and oxygen were observed [6, 25, 59]. The CKa peak was also detected. This carbon
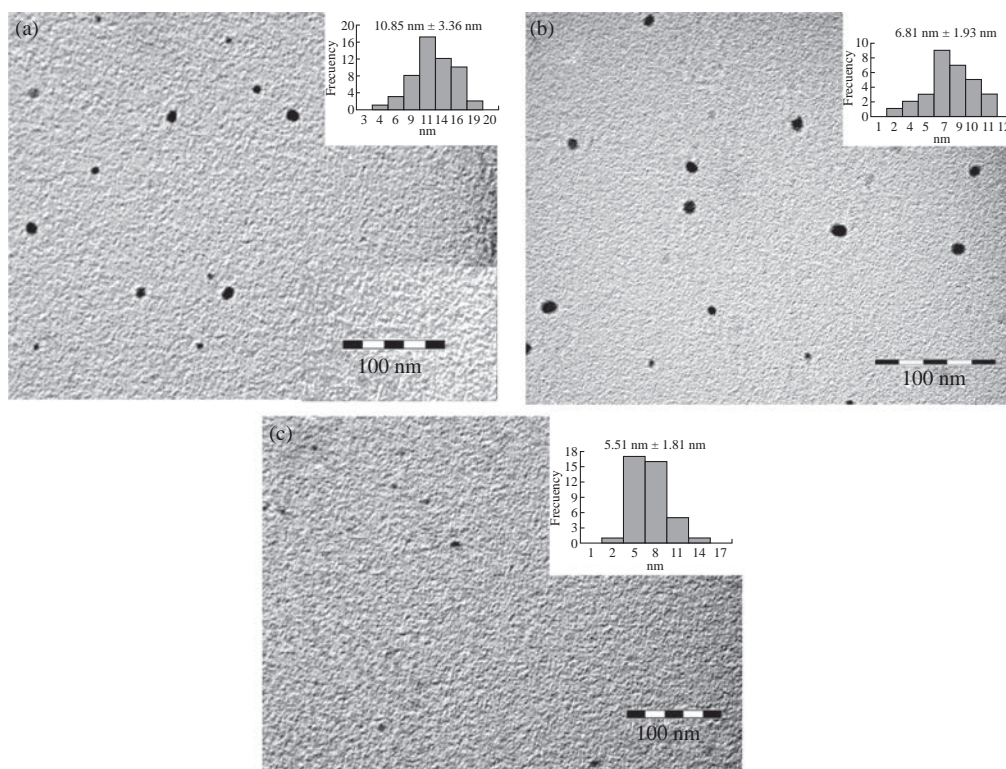

Fig. 3 TEM images and particle size distribution of Cu_2O nanoparticles prepared at different ratios of $[Cu^{2+}] : [N_2H_4]$ at **(a)** 2 : 3, **(b)** 4 : 7 and **(c)** 2 : 5.

398

Nano Biomed. Eng., 2018, Vol. 10, Iss. 4

Table 2 Mean diameter of each sample obtained by chemical reaction (PVP = 0.50% (v/v); EDTA (1.0 mM); KOH (2.0 mM))

Sample	Crystalline feature	Mean diameter (nm)	Distribution (nm)
MH01	Cu_2O	10.85 ± 3.36	3.59-19.83
MH02	Cu_2O	6.81 ± 1.93	1.38-11.52
MH03	Cu_2O	5.51 ± 1.81	1.42-15.17
MB01	CuO	4.99 ± 1.41	2.38-9.06
MBP01	CuO	4.49 ± 1.21	1.65-7.47
MB02	CuO and Cu_2O	2.81 ± 0.66	1.28-4.19
MB03	CuO and Cu_2O	6.79 ± 1.81	3.17-12.61
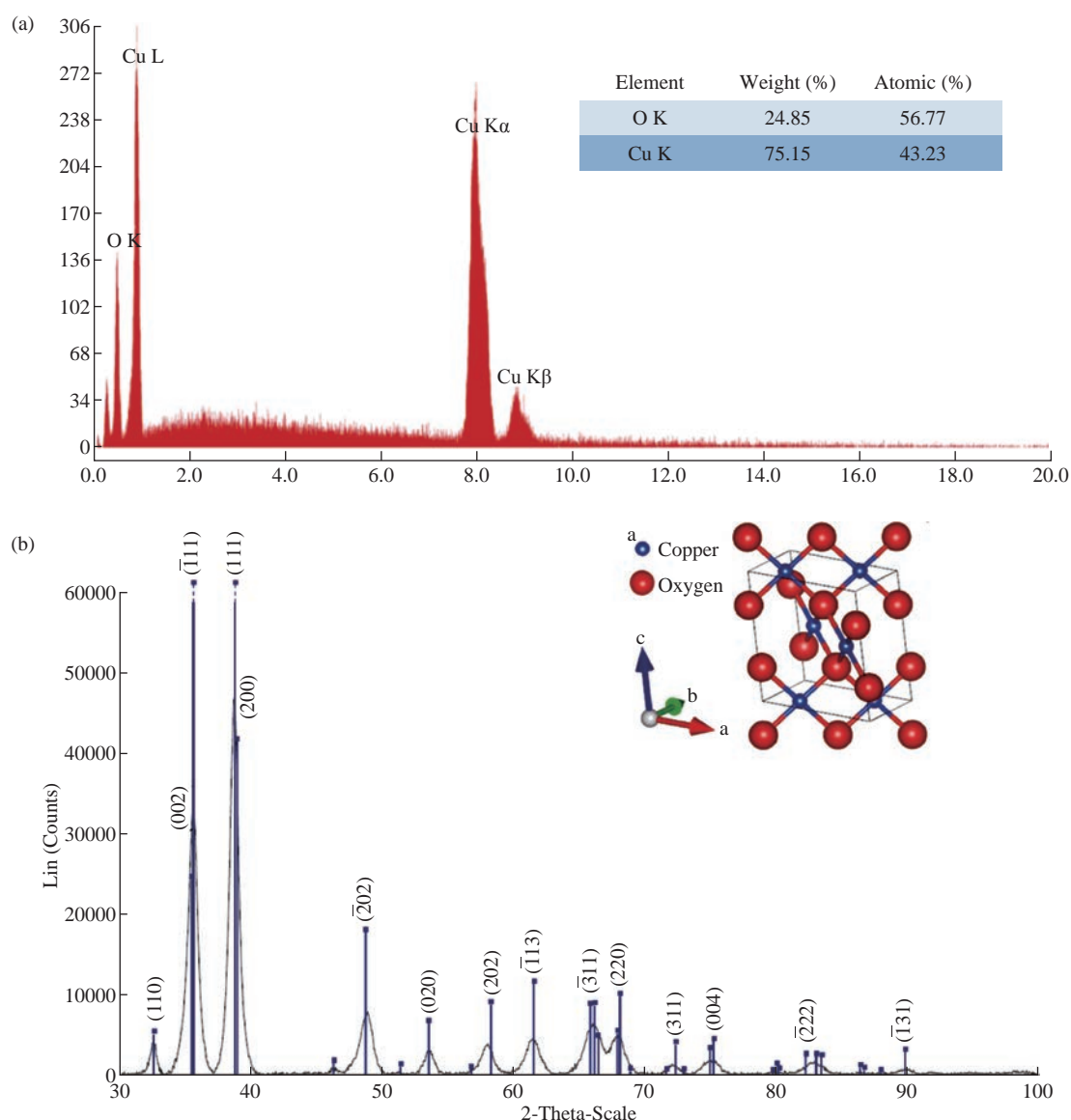
Fig. 4 (a) EDS spectrum of sample copper oxide nanoparticles, $[Cu^{2+}] : [NaBH_4] = 2 : 1$; **(b)** XRD patterns of Cu_2O nanoparticles prepared with sodium borohydride, $[Cu^{2+}] : [NaBH_4] = 2 : 1$.

peak was due to the SEM holding sample. No other obvious peak belonging to impurity was detected. This result indicated that the as-synthesized product was composed of high-purity copper oxide NPs. A similar EDS spectra were obtained for the rest of samples prepared. The XRD spectra (Fig. 4(b)) for samples prepared with sodium borohydride at low concentrations confirmed the formation of cupric

Nano Biomed. Eng., 2018,Vol. 10, Iss. 4

399

oxide The diffraction peaks in each pattern could be well indexed to the phase of cupric oxide (CuO) with monoclinic structure of tenorite (JCPDS card no.00-41-254) with lattice parameters a = 4.68 Å, b = 3.42 Å, c = 5.12 Å and β = 99.42°. This result was in agreement with studies previously reported [12, 22-23, 29, 41-43, 59-60]. In addition, Fan et al. [38] reported that $NaBH_4$ acted as both alkaline agent and reductant for the growth of unusual CuO structures.

This result was confirmed by the corresponding HEED pattern of NPs shown on the right-hand illustration in Fig. 5 (sample MB01). When the electron diffraction was carried out on a limited number of crystals, only some spots of diffraction distributed in concentric circles were observed. The ring patterns of sample MB01 with plane distances of 2.52 Å, 2.32 Å, 1.87 Å, 1.58 Å, 1.41 Å, and 1.37 Å were consistent with the plane families (11), (111), (02), (202), (11) and (220) of single-phase CuO with a monoclinic structure [31, 43, 61] This result led us to thinking that copper NPs previously obtained (Equations (2), (3) and (4)) could be immediately oxidized to cupric oxide (CuO) according to Equation (6). Additionally, if any amount of cuprous oxide (Cu_2O) NPs is obtained, under the given conditions, they will be oxidized to cupric oxide (CuO) according to Equation (8). Furthermore, based on the elemental analysis of sample MB01 (Cu=81.87%, O=18.13%), the weight Cu:O ratio could be calculated to be 4.52, which was close to theoretical value of 4 for CuO. The results of EDS analysis confirmed that the produced nanopowder was CuO, which was in agreement with the results of XRD.

The corresponding XRD pattern of samples MB01, MBP01, MB02 and MB03 are shown in Fig. 6. This figure shows the XRD analysis results for the four different operating sodium borohydride concentrations. Fig. 6 shows XRD patterns with a predominant presence of CuO with traces of Cu_2O. The peak of CuO was observed in all samples. However, peaks corresponding to Cu_2O were identified for samples MB02 and MB03. As sodium borohydride ($NaBH_4$) concentration increased cuprous oxides formation was favored. These results suggested the formation of Cu_2O and CuO in colloidal solution, which was in agreement with results previously reported [43, 62-64]. One explanation for these results is the high activity of copper NPs which are obtained during the synthesis. Due to their small size and higher surface area, they have a high oxidation susceptibility of copper oxide (+1) and copper oxide (+2) according to Equation (5) and (6). Also, a simultaneous oxidation reaction of cuprite to tenorite can be carried out according to Equation (8). In addition, as Yagi [34] and Zhang et al. [55] reported, it was possible to obtain cuprite using $NaBH_4$ as the reducing agent if a suitable volume of PVP was used (Equation 11). A similar X-ray spectrum of NPs indicating the presence of two crystalline phases, monoclinic cupric oxide (CuO) and cubic cuprous oxides (Cu_2O) was reported by Abboud et al. [64].

The size and the morphology of copper oxide NPs were analyzed by TEM. Fig. 7 show the morphology and the particle size distribution of copper oxide NPs when different volumes of $NaBH_4$ as a reductant agent
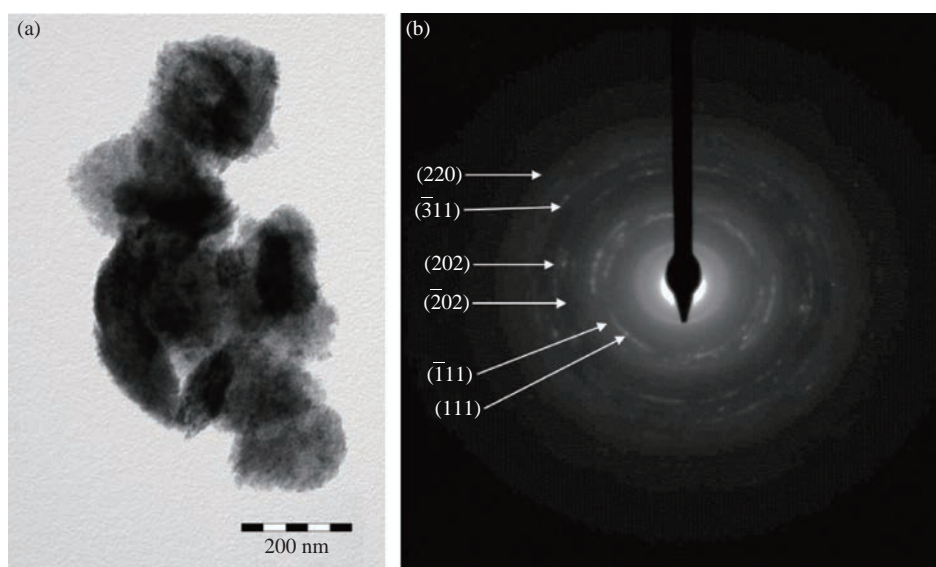

Fig. 5 (a) TEM image and **(b)** HEED of agglomerates Cu_2O nanoparticles prepared with sodium borohydride, $[Cu^{2+}] : [NaBH_4] = 2 : 1$.

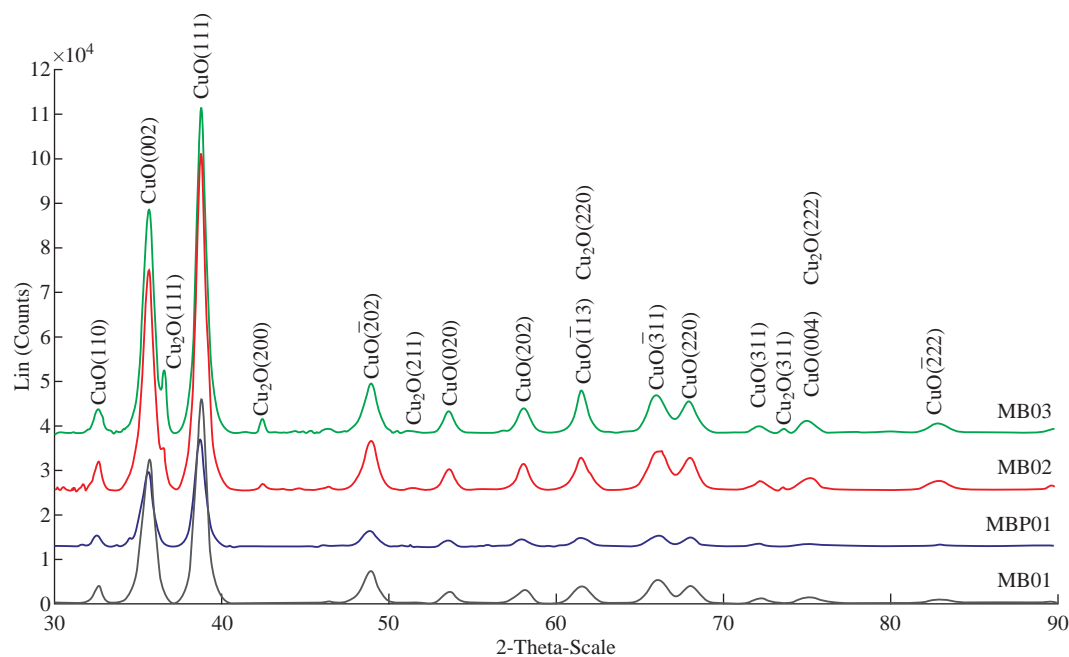400

Nano Biomed. Eng., 2018, Vol. 10, Iss. 4

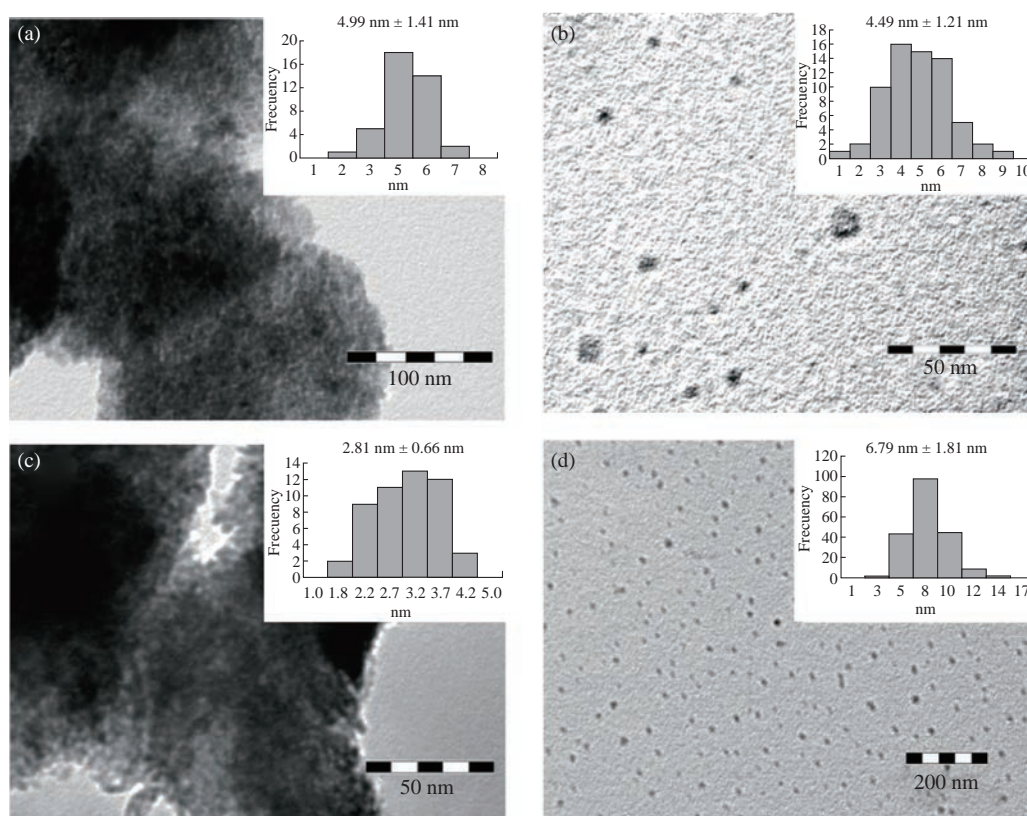**Fig. 6** XRD patterns of copper oxide nanoparticles prepared at different amounts of sodium borohydride.

Fig. 7 TEM images and particle size distribution of CuO nanoparticles prepared at different ratios of $[Cu^{2+}] : [NaBH_4]$ at **(a)** 2 : 1, **(b)** 4 : 3, **(c)** 1 : 1 and **(d)** 1 : 2.

were used. Well dispersed and semispherical NPs are observed in Fig. 7(b) and (d). In contrast, agglomerates of very small NPs are seen in Fig. 7(a) and (c). The spherical shape is in concordance with results previously reported [27, 30, 33, 43, 45, 59]. On the

right hand of Fig. 7, the size distribution histograms of colloidal CuO NPs of samples MB01, MBP01, MB02 and MB03 is presented. NPs ranging from 2.38 to 9.06 nm, 1.65 to 7.47 nm, 1.28 to 4.19 nm and 3.17 to 12.61 nm can be observed respectively. The estimated

Nano Biomed. Eng., 2018, Vol. 10, Iss. 4

401

mean diameter was 4.99 ± 1.41 nm, 4.49 ± 1.21 nm, 2.81 ± 0.66 nm and 6.79 ± 1.81 nm. Similar results were reported by Sahooli et al. [29]. The crystallite mean diameter estimated by Scherrer's formula from the XRD pattern was 14.45, 14.92, 14.62 and 15.27 nm. Spherical CuO NPs with similar mean diameters were reported previously [7, 27, 29, 31, 33, 65]. The results showed that as the NaBH$_4$ volume increased, the nucleation process was favored until the critical radius was reached, and therefore mean size of the NPs decreased. However, when the volume of NaBH$_4$ was twice that of Cu^{2+}, the NPs mean size increased dramatically because the growth process was favored. Likewise, this result may be due to the process of ripening of particles as described by Oswald [66, 67].

Antibacterial activity

The antimicrobial susceptibility of copper oxide NPs synthesized was investigated. The Kirby-Bauer diffusion method was used as antimicrobial susceptibility testing method to determine if the strain was resistant, intermediate, or susceptible to the antibiotics tested. Gram-positives *Staphylococcus aureus strain* (CCM 3953) *and Staphylococcus aureus MRSA strain* (ATCC 9027), and Gram-negatives *Escherichia coli strain* (ATCC 10536)

and Pseudomonas aeruginosa strain (ATCC 10145) were used as the bacilli. The four samples of NPs tested had the same morphology, but different composition. Sample MH02 was cuprite, sample MBP01 was tenorite, while samples MB02 and MB03 were principally tenorite and with the presence of some cuprite. The average particle sizes used for the antibacterial test were 6.81 ± 1.93 nm, 4.49 ± 1.21 nm, 2.81 ± 0.66 nm and 6.79 ± 1.81 nm, respectively.

Disposable plates inoculated with the tested Gram-positive and Gram-negative bacteria at a concentration of 10^5 to 10^6 CFU/mL were used for the tests. Copper oxide NPs sols were inoculated in the disposable plates containing Gram-positive and Gram-negative bacteria. Zones of inhibition were measured after 24 h of incubation at 35 °C. The diameter of inhibition zones (in millimeters) measured is shown in Table 3. The clear zone diameter of the bacterial inhibition zone was correlated to antibiotic activity - vancomycin and gentamicin - for Gram-positive and Gram-negative bacteria, respectively. Sample MH02 composed of cuprite did not show any positive results.

Comparing the gram-negative bacteria, the inhibition zone remains almost constant for the *E. coli* strain when different samples of NPs were used (Fig.

Table 3 Zone of inhibition (mm) of copper oxide nanoparticles sols against test strains

Sample	MH02	MBP01	MB02	MB03
Crystalline feature	Cu$_2$O	CuO	CuO and Cu$_2$O	CuO and Cu$_2$O
Mean diameter (nm)	6.81 ± 1.93	4.49 ± 1.21	2.81 ± 0.66	6.79 ± 1.81
E. coli ATCC 10536	--	14	15	14
P. aeruginosa ATCC 10145	--	17	22	23
S. aurus CCM 3953	--	19	18	22
S. aurus MRSA ATCC 9027	--	22	20	22
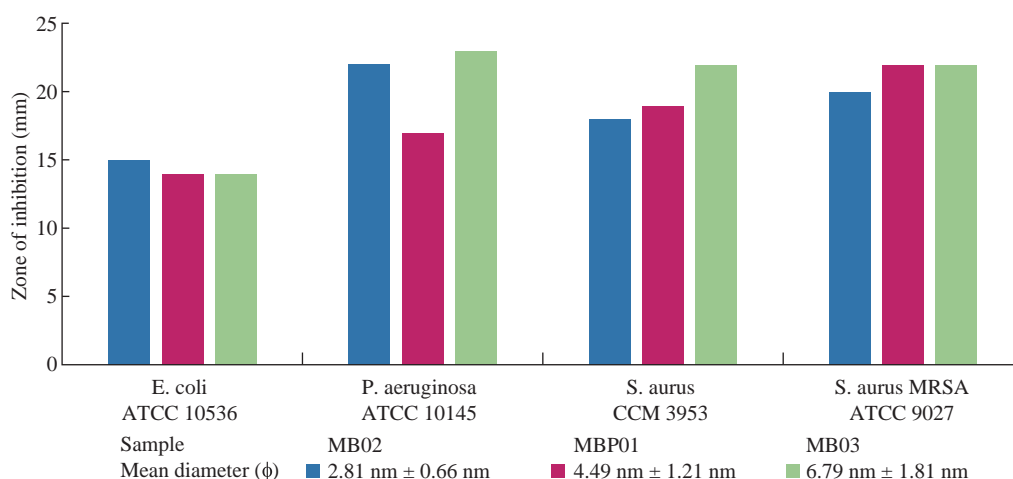
Fig. 8 Diffusion assay of copper oxide nanoparticles against microbial strains.

402

Nano Biomed. Eng., 2018, Vol. 10, Iss. 4

8). Comparable results were reported by Abboud et al. [64] and Azam et al. [12, 68] using NPs of CuO with 20-22 nm and 5-45 nm of mean size respectively. Diameters of the inhibition zone were greater in the case of *P. aeruginosa* when MB02 and MB03 were tested. Azam et al. [68] reported similar diameter of the inhibition zone In this case, the presence of cuprite seemed to improve the inhibition of the bacteria even for the larger NPs. In the case of the *S. aureus*, a smaller diameter of inhibition zone was observed for the sample MB02 that showed the smallest mean NP size. The highest inhibition zone was reported for sample MB03, suggesting that the presence of Cu_2O had a positive effect on bacterial inhibition [64]. A similar behavior was observed for *S. aureus* MRSA strain, although in this case the diameter of the inhibition zone was slightly higher. NPs of cuprite (Cu_2O) did not show bacteriological activity in any case. The interaction between Gram-positive bacteria and NPs seemed stronger than that of Gram-negative bacteria because of the difference in cell walls between both bacteria. The cell wall of *E. coli* and *P. auriginosa* consisted of lipids, proteins and lipopolysaccharides (LPS), providing effective protection against biocides. However, the cell wall of Gram-positive bacteria, such as *S. aureus* and *S. aurus MRSA,* did not consist of LPS [18]. The results of bacterial susceptibility were encouraging, given that the antibacterial behavior was comparable to those of silver NPs previously reported [2]. However, it is necessary to determine the minimum inhibitory concentration de MIC of each sample.

It is possible that copper oxide NPs act as the antimicrobial agents for the treatment of bacterial infections [13, 14]. Though, the mechanism of the bactericidal effect of copper oxide colloid NPs against bacteria is not clear. One of the possible reasons for this could be the direct interaction between copper oxide NPs and external membrane surface of the bacteria. In this context, a number of mechanisms have been proposed to interpret the antibacterial behavior of metal oxides [5].

Different ways of action of copper oxide NPs have been proposed by Pena et al. [69] and Kim et al. [70]. Copper ions released may also interact with DNA molecules and intercalate with nucleic acid strands. In addition, copper ions released subsequently may bind with DNA molecules and lead to disorder of the helical structure by cross-linking within and between the nucleic acid strands. Copper oxides generate reactive hydroxyl radicals oxidize proteins, cleavage DNA and RNA molecules and damage membrane due to oxidation of the lipid [18]. Copper ions inside bacteria cells also disrupt biochemical processes [69]. Also, oxygen free-radical created from excited electrons of Cu_2O particles surface are powerful oxidizing agents,
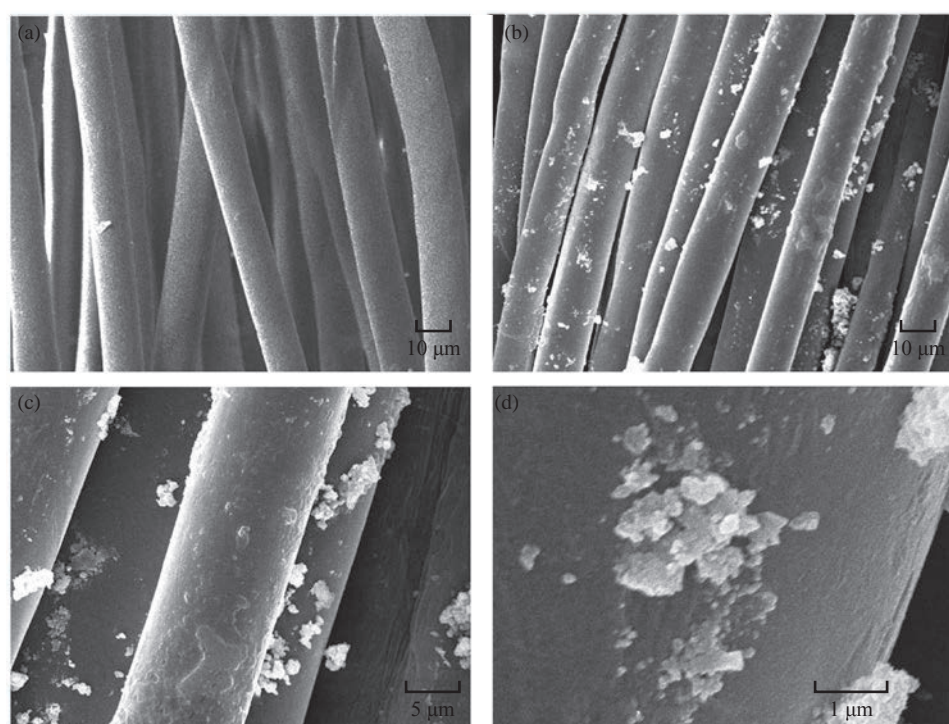

Fig. 9 SEM images of **(a)** blank cotton, **(b)** washed cotton, **(c)** nanoparticles of CuO-coated cotton by ultrasound waves, and **(d)** nanoparticles of CuO-coated cotton in zoom images.

breaking the cell wall of microorganisms through oxidation–reduction reactions [70]. However, the precise mechanism of action of nano CuO is the subject of ongoing investigations. The antibacterial effect of copper oxide NPs determined in this study was similar to that in previous reports [7, 10, 12, 64, 68].

Coating cotton fabric

Finally, copper oxide NPs with bactericidal activity, sample MBP01 were incorporated into cotton fabrics (11.8 cm^2) by applying ultrasound waves. The morphology of the fiber surface area before and after deposition of CuO NPs was studied by SEM (Fig. 9). On the SEM image of the original cotton fiber (Fig. 9(a)), grooves and fibrils could be easily observed on the surface of the fiber. SEM images of CuO NPs coated onto cotton fibers at different zoom are presented in Fig. 9(c) and (d). It was clear that cotton fibers were covered homogeneously with CuO NPs when ultrasounds waves were used. However, some agglomerated were observed.

The impregnated cotton fabric was washed in order to reveal whether the particles were well fixed in the fabric or not. After those fabrics were washed five times in a mini washing machine with ultrapure water (Millipore Inc.), remains of copper oxide NPs were evaluated by atomic absorption spectroscopy AAS. Fabrics impregnated with ultrasound waves after five washes retained 95% of the copper oxide NPs (Fig. 9(b)). Then, NPs were strongly physically adsorbed onto the cotton substrate when ultrasound waves were used, since these particles were not removed by several washings. In concordance of the antibacterial activity, these materials can be used as antibacterial fabrics in the form of medical cloths, protective garments and bed spreads, and many other purposes to minimize the chance of nosocomial infections, though antibacterial test was still under way.

Conclusions

Cupric and cuprous oxide NPs have been successfully synthesized using copper sulfate as precursor, with sodium borohydride (NaBH$_4$) and hydrazine (N$_2$H$_4$) as reducing agents, respectively. The EDS of the NPs dispersion confirmed the presence of elemental copper and oxygen signals. No elemental impurity was detected. Effects of the influential parameters as type and concentration of reducing agent were investigated. XRD confirmed that Tenorite (CuO) and cuprite NPs (Cu$_2$O) were obtained when different

ratios of CuSO$_4$/NaBH$_4$ and CuSO$_4$/N$_2$H$_4$ were used respectively.

TEM images showed that the products were composed of semispherical particles with narrow size distribution and high dispersion. It was possible to obtained NPs of CuO and Cu$_2$O from a simple method of chemical reduction with the mean size from 2 to 20 nm. The influence of the ratio of copper sulfate and reductant agent on the NPs mean size was most evident when hydrazine hydrate (N$_2$H$_4$) was used. The decrease in size of the Cu$_2$O NPs was observed when the amount of hydrazine increased. This may be due to the availability of more nucleation sites and lower growth rate for Cu$_2$O NPs.

Additionally, the antibacterial activity of the nanopartículas dispersion was measured by the Kirby-Bauer method. The results of this study clearly demonstrated that the colloidal copper oxide NPs inhibited the growth and multiplication of the tested bacteria, including highly multiresistant bacteria such as methicillin-resistant *Staphylococcus aureus*, *S. aureus, Escherichia coli* and *Pseudomonas aeruginosa.* The results suggested that CuO was responsible for bacterial activity even in the presence of small amounts of Cu$_2$O. *Pseudomonas aureginosa and Staphylococcus aureus* were more susceptible to the particle size than *Escherichia coli*. NPs of cuprite (Cu$_2$O) did not show bacteriological activity in any case. The standard dilution micro method, determining the minimum inhibitory concentration (MIC) leading to inhibition of bacterial growth was under way.

The use of ultrasound waves allowed a stronger adhesion of NPs to fabrics. The NPs were retained onto cotton fibber even after five washes.

Acknowledgments

Conflict of interest

The authors declare that they have no conflict of interest in the publication.

References

[1]   S. Pal, Y.K. Tak, and J.M. Song, Does the Antibacterial

404

Nano Biomed. Eng., 2018, Vol. 10, Iss. 4

Activity of Silver Nanoparticles Depend on the Shape of the Nanoparticle? A Study of the Gram-Negative Bacterium Escherichia coli. *Applied and Environmental Microbiology*, 2007, 73: 1712-1720.

[2] M. Guzman, J. Dille, and S. Godet, Synthesis and antibacterial activity of silver nanoparticles against gram-positive and gram-negative bacteria. *Nanomedicine: Nanotechnology, Biology, and Medicine*, 2012, 8: 37-45.

[3] J. Ramyadevi, K. Jeyasubramanian, A. Marikani, et al., Synthesis and antimicrobial activity of copper nanoparticles. *Materials Letters*, 2012, 71: 114-116.

[4] C.H. Lu, L.M. Qi, J.H. Yang, et al., Simple template-free solution route for the controlled synthesis of $Cu(OH)_2$ and CuO nanostructures. *J. Phys. Chem. B*, 2004, 108: 17825-17831.

[5] D. Das, B.Ch. Nath, P. Phukon, et al., Synthesis and evaluation of antioxidant and antibacterial behavior of CuO nanoparticles. *Colloids and Surfaces B: Biointerfaces*, 2013, 101: 430-433.

[6] C. Karunakaran, G. Manikandan, and P. Gomathisankar, Microwave, sonochemical and combustion synthesized CuO nanostructures and their electrical and bactericidal properties. *Journal of Alloys and Compounds*, 2013, 580: 570-577.

[7] S. Jadhav, S. Gaikwad, M. Nimse, et al., Copper oxide nanoparticles: synthesis, characterization and their antibacterial activity. *J. Clus Sci.*, 2011, 22: 121-129.

[8] I.M. El-Nahhal, S.M. Zourab, F.S. Kodeh, et al., Nanostructured copper oxide-cotton fibers: synthesis, characterization, and applications. *International Nano Letters*, 2012, 2: 1-5.

[9] A.Y. Booshehri, R. Wang, and R. Xu, Simple method of deposition of CuO nanoparticles on a cellulose paper and its antibacterial activity. *Chemical Engineering Journal*, 2015, 262: 999-1008.

[10] R. Naika, K. Lingaraju, K. Manjunath, et al., Green synthesis of CuO nanoparticles using Gloriosa superba L. extract and their antibacterial activity. *Journal of Taibah University for Science*, 2015, 9: 7-12.

[11] O. Mahapatra, M. Bhagat, C. Gopalakrishnan, et al., Ultrafine dispersed CuO nanoparticles and their antibacterial activity. *Journal of Experimental Nanoscience*, 2008, 3: 185-193.

[12] A. Azam, A.S. Ahmed, M. Oves, et al., Antimicrobial activity of metal oxide nanoparticles against Gram-positive and Gram-negative bacteria: A comparative study. *International Journal of Nanomedicine*. 2012, 7: 6003-6009.

[13] V.R. Rai, A.J. Bai, Nanoparticles and their potential application as antimicrobials, Science against microbial pathogens: communicating current research and technological advances. *Microbiology Series*, 2011, 3: 197-209.

[14] G. Ren, D. Hu, E. Cheng, et al., Characterisation of copper oxide nanoparticles for antimicrobial applications. *International Journal of Antimicrobial Agents*, 2009, 33: 587-590.

[15] L. Otero-Gonzalez, J.A. Field, and R. Sierra-Alvarez, Inhibition of anaerobic wastewater treatment after long-term exposure to low levels of CuO nanoparticles. *Water Research*, 2014, 58: 160-168.

[16] A. Sedighi, M. Montazer, and N. Samadi, Synthesis of nano Cu_2O on cotton: Morphological, physical, biological and optical sensing characterizations. *Carbohydrate Polymers*, 2014, 110: 489-498.

[17] Clinical and Laboratory Standards Institute, Performance standards for antimicrobial disk and dilution susceptibility test: M2-A9. Performance standards for antimicrobial susceptibility testing. 18th informational supplement: M100-S18. 2008.

[18] G. Speranza, G. Gottardi, C. Pederzolli, et al., Role of chemical interactions in bacterial adhesion to polymer surfaces. *Biomaterials*, 2004, 25: 2029-2037.

[19] B. Khodashenas, H.R. Ghorbani, Synthesis of copper nanoparticles: An overview of the various methods. *Korean J. Chem. Eng.*, 2014, 31: 1105-1109.

[20] M. Salavati-Niasari, F. Davar, Synthesis of copper and copper(I) oxide nanoparticles by thermal decomposition of a new precursor. *Materials Letters*, 2009, 63: 441-443.

[21] L.J. Zhou, Y.C. Zou, J. Zhao, et al., Facile synthesis of highly stable and porous Cu_2O/CuO cubes with enhanced gas sensing properties. *Sensors and Actuators B.*, 2013, 188: 533-539.

[22] H. Fan, L. Yang, W. Hua, et al., Controlled synthesis of monodispersed CuO nanocrystals. *Nanotechnology*, 2004, 15: 37-42.

[23] A. Shuin, W. Zhu, L. Xu, et al., Green sonochemical synthesis of cupric and cuprous oxides nanoparticles and their optical properties. *Ceramics International*, 2013, 39: 8715-8722.

[24] K. Borgohain, N. Murase, and S. Mahamuni, Synthesis and properties of Cu_2O quantum particles. *J. Appl. Phys.*, 2002, 92: 1292-1297.

[25] P. Pandey, S. Merwyn, G.S. Agarwal, et al., Electrochemical synthesis of multi-armed CuO nanoparticles and their remarkable bactericidal potential against waterborne bacteria. *Journal of Nanopart Res.*, 2012, 14: 1-13.

[26] S. Dagher, Y. Haik, A.I. Ayesh, et al., Synthesis andoptical properties of colloidal CuO nanoparticles. *Journal of Luminescence*, 2014, 151: 149-154.

[27] H. Wang, J.Z. Xu, J.J. Zhu, et al., Preparation of CuO nanoparticles by microwave irradiation. *Journal of Crystal Growth*, 2002, 244: 88-94.

[28] C. Yang, X. Su, J. Wang, et al., Facile microwave-assisted hydrothermal synthesis of varied-shaped CuO nanoparticles and their gas sensing properties. *Sensors and Actuators B.*, 2013, 185:159-165.

[29] M. Sahooli, S. Sabbaghi, and R. Saboori, Synthesis and characterization of mono sized CuO nanoparticles. *Materials Letters*, 2012, 81: 169-172.

[30] J. Pike, F.S.W. Chan, F. Zhang, et al., Formation of stable Cu_2O from reduction of CuO nanoparticles. *Applied Catalysis A: General*, 2006, 303: 273-277.

[31] A. El-Trass, H. El-Shamy, I. El-Mehasseb, et al., CuO nanoparticles: Synthesis, characterization, optical properties and interaction with amino acids. *Applied Surface Science*, 2012, 258: 2997-3001.

[32] K. Phiwdanga, S. Suphankij, W. Mekprasart, et al., Synthesis of CuO Nanoparticles by Precipitation Method Using Different Precursors. *Energy Procedia*, 2013, 34: 740-745.

[33] J. Zhu, D. Li, H. Chen, et al., Highly dispersed CuO nanoparticles prepared by a novel quick-precipitation method. *Materials Letters*, 2004, 58: 3324-3327.

[34] S. Yagi, Potential-pH diagrams for oxidation-state control of nanoparticles synthesized via chemical reduction. *Thermodynamics - physical chemistry of aqueous systems.* InTech, 2011: 223-239.

[35] S. Arshadi-Rastabi, J. Moghaddam, and M. Reza, Synthesis, characterization and stability of Cu_2O nanoparticles produced via supersaturation method considering operational parameters effect. *Journal of Industrial and Engineering Chemistry*, 2015, 22: 34-40.

[36] L. Yuan, Q. Yin, Y. Wang, et al., CuO reduction induced formation of CuO/Cu_2O hybrid oxides. *Chemical Physics Letters*, 2013, 590: 92-96.

[37] D. Dodoo-Arhin, M. Leoni, P. Scardi, et al., Synthesis, characterisation and stability of Cu_2O nanoparticles produced via reverse micelles microemulsion. *Materials*

Nano Biomed. Eng., 2018, Vol. 10, Iss. 4

405

Chemistry and Physics, 2010, 122: 602-608.

[38] G. Fan, F. Li, Effect of sodium borohydride on growth process of controlled flower-like nanostructured Cu_2O/CuO films and their hydrophobic property. *Chemical Engineering Journal*, 2011, 167: 388-396.

[39] J. Zhu, H. Bi, Y. Wang, et al., Solution-phase synthesis of Cu_2O cubes using CuO as a precursor. *Materials Letters*, 2008, 62: 2081-2083.

[40] M. Srivastava, J. Singh, R.K. Mishra, et al., Electro-optical and magnetic properties of monodispersed colloidal Cu_2O nanoparticles. *Journal of Alloys and Compounds*, 2013, 555: 123-130.

[41] D. Han, H. Yang, Ch. Zhu, et al., Controlled synthesis of CuO nanoparticles using TritonX-100-based water-in-oil reverse micelles. *Powder Technology*, 2008, 185: 286-290.

[42] R. Etefagh, E. Azhir, and N. Shahtahmasebi, Synthesis of CuO nanoparticles and fabrication of nanostructural layer biosensors for detecting Aspergillus niger fungi. *Scientia Iranica F.*, 2013, 20: 1055-1058.

[43] X. Liu, B. Geng, Q. Du, et al., Temperature-controlled self-assembled synthesis of CuO, Cu_2O and Cu nanoparticles through a single-precursor route. *Materials Science and Engineering A.*, 2007, 448: 7-14.

[44] W. Lee, L. Piao, Ch. Park, et al., Facile synthesis and size control of spherical aggregates composed of Cu_2O nanoparticles. *Journal of Colloid and Interface Science*, 2010, 342: 198-201.

[45] P. He, X. Shen, and H. Gao, Size-controlled preparation of Cu_2O octahedron nanocrystals and studies on their optical absorption. *Journal of Colloid and Interface Science*, 2005, 284: 510-515.

[46] L. Qing-ming, Z. De-bi, Y.Y. Yamamoto, et al., Effects of reaction parameters on preparation of Cu nanoparticles via aqueous solution reduction method with $NaBH_4$. *Trans. Nonferrous Met. Soc. China*, 2012, 22: 2991-2996.

[47] S.M. Badawy, R.A. El-Khashab, and A.A. Nayl, Synthesis, characterization and catalytic activity of Cu/Cu_2O nanoparticles prepared in aqueous medium. *Bulletin of Chemical Reaction Engineering & Catalysis*, 2015, 10: 169-174.

[48] P.J. Chen, L.L. Lim, Key factors in chemical reduction by hydrazine for recovery of precious metals. *Chemosphere*, 2002, 49: 363-370.

[49] H. Zhao, J. Yang, L. Wang, et al., Fabrication of a palladium nanoparticle/graphene nanosheet hybrid via sacrifice of a copper template and its application in catalytic oxidation of formic acid. *Chem. Commun.*, 2011, 47: 2014-2016.

[50] J.C. Fanning, B.C. Brooks, A.B. Hoeglund, et al., The reduction of nitrate and nitrite ions in basic solution with sodium borohydride in the presence of copper(II) ions. *Inorganica Chimica Acta*, 2000, 310: 115-119.

[51] C. Gomez-Lahoz, F. Garcia-Herruzo, J.M. Rodriguez-Maroto, et al., Cobalt (II) removal from water by chemical reduction with sodium borohydride. *War. Res.*, 1993, 27: 985-992.

[52] F. Burriel, F. Lucena, S. Arribas, et al., *Qualitative analytical chemistry*, 18ª ed. Thomson Paraninfo, Madrid (Spain), 2006.

[53] D. Chen, S. Ni, J.J. Fang, et al., Preparation of Cu_2O nanoparticles in cupric chloride solutions with a simple mechanochemical approach. *Journal of Alloys and Compounds*, 2010, 504: S345-S348.

[54] A. Muramatsu, T. Sugimoto, Synthesis of uniform spherical Cu_2O particles from condensed CuO suspensions. *Journal of Colloid and Interface Science*, 1997, 189: 167-173.

[55] J. Zhang, J. Liu, Q. Peng, et al., Nearly monodisperse Cu_2O and CuO nanospheres: Preparation and applications for sensitive gas sensors. *Chem. Mater*, 2006, 18: 867-871.

[56] Y.X. Wang, X.F. Tang, and Z.G. Yang, A novel wet-chemical method of preparing highly monodispersed Cu_2O nanoparticles. *Colloids and Surfaces A: Physicochem. Eng. Aspects*, 2011, 388: 38-40.

[57] V.K. LaMer, R.H. Dinegar, Theory, production and mechanism of formation of monodispersed hydrosols. *J. Am. Chem. Soc.*, 1950, 72: 4847-4854.

[58] V.K. LaMer, Nucleation in phase transitions. *Ind. Eng. Chem.*, 1952, 44(6): 1270-1277.

[59] E. Darezereshki, F. Bakhtiari, A novel technique to synthesis of tenorite (CuO) nanoparticles from low concentration $CuSO_4$ solution. *J. Min. Metall. Sect. B-Metall*, 2011, 47: 73-78.

[60] G. Isani, M.L. Falcioni, G. Barucca, et al., Comparative toxicity of CuO nanoparticles and $CuSO_4$ in rainbowtrout. *Ecotoxicology and Environmental Safety*, 2013, 97: 40-46.

[61] B.G. Ganga, P.N. Santhosh, Manipulating aggregation of CuO nanoparticles: Correlation between morphology and optical properties. *Journal of Alloys and Compounds*, 2014, 612: 456-464.

[62] M. Yin, C.K. Wu, Y. Lou, et al., Copper oxide nanocrystals. *J Am Chem Soc*, 2005, 127: 9506-9511.

[63] A. Rahman, A. Ismail, D. Jumbianti, et al., Synthesis of copper oxide nanoparticles by using *Phormidium cyanobacterium*. *Indo J Chem*, 2009, 9: 355-360.

[64] Y. Abboud, T. Saffaj, A. Chagraoui, et al., Biosynthesis, characterization and antimicrobial activity of copper oxide nanoparticles (CONPs) produced using brown alga extract (Bifurcaria bifurcata). *Applied Nanoscience*, 2014, 4: 571-576.

[65] M. Estruga, A. Roig, C. Domingo, et al., Solution-processable carboxylate-capped CuO nanoparticles obtained by a simple solventless method. *J Nanopart Res.*, 2012, 14: 1-9.

[66] W. Ostwald, Über die vermeintliche Isomerie des roten und gelben Quecksilberoxyds und die Oberflächenspannung fester Körper [Supposed isomerism of the red and yellow mercuric oxide and the surface tension of solid bodies]. *Z. Phys. Chem.*, 1900, 34: 495-503.

[67] N.T.K. Thanh, N. Maclean, and S. Mahidd, Mechanisms of nucleation and growth of nanoparticles in solution. *Chem. Rev.*, 2014, 114: 7610-7630.

[68] A. Azam, A.S. Ahmed, M. Oves, et al., Size-dependent antimicrobial properties of CuO nanoparticles against Gram-positive and -negative bacterial strains. *International Journal of Nanomedicine*, 2012, 7: 3527-3535.

[69] M.M.O. Pena, K.A. Koch, and D.J. Thiele, Dynamic regulation of copper uptake and detoxification genes in Saccharomyces cerevisiae. *Molecular and Cellular Biology*, 1998, 18: 2514-2523.

[70] J.H. Kim, H. Cho, S.E. Ryu, et al., Effects of metals ions on the activity of protein tyrosine phosphate VHR: Highly potent and reversible oxidative inactivation by Cu_2O ion. *Archives of Biochemistry and Biophysics*, 2000, 382: 72-80.